Excited States and Rydberg Series in the Emission Spectrum of NO

by **Martin Huber**

Institute of Physics of the University of Basel, Switzerland

(19. XII. 63)

Abstract: The emission spectrum of nitric oxide (NO) has been photographed in the visible (5150 to 6900 Å) and infrared (7625 to 11000 Å) regions, using the large dispersion of an 11 m grating spectrograph in the second (0.7 Å/mm) and first (1.4 Å/mm) order, respectively. The light source was an electric discharge through a rapidly streaming mixture of NO and A gas.

Rotational analyses are given for the $H\,^2\Sigma^+$, $H'\,^2\Pi$–$D\,^2\Sigma^+$ (0,0) and (1,1); $H\,^2\Sigma^+$–$A\,^2\Sigma^+$ (0,0) and (1,1); $H\,^2\Sigma^+$, $H'\,^2\Pi$–$C\,^2\Pi$ (0,0); $F\,^2\Delta$–$C\,^2\Pi$ (0,0); $B'\,^2\Delta_i$–$C\,^2\Pi$ (4,1) and for the $B'\,^2\Delta_i$–$B\,^2\Pi$ (1,0) and (2,0) bands. Previous assignments are confirmed. Results are obtained for the Δ-Δ perturbation between the F and B' states. The constant p of Λ-type doubling in the $B\,^2\Pi$ state is determined.

Intensity anomalies occuring in bands in which H and H' states are involved are explained. An interpretation is suggested of previously unassigned bands as higher members of Rydberg series.

I. Introduction

§ 1. The visible part of the NO emission spectrum, which is produced by an electric discharge in a fast stream of NO or NO_2 gas at relatively high pressure, was first described by GEHLHOFF[1]) (1907) and photographed later by ZENNECK and STRASSER[2]); the first exposures in the photographic infrared are due to FEAST[3]) (1950). HEATH[4]) (1960) extended the investigation into the PbS region. Recently the spectrum around 11000 Å was observed in shock waves in air[5]).

The fine structure of the $B'\,^2\Delta$ – $B\,^2\Pi$ bands (BAER and MIESCHER[6])) which are shaded to the violet and are arranged in several groups, has not been investigated before. Moreover, there are several bands which are neither shaded nor seem to belong to a group. Of these only the $E\,^2\Sigma^+$–$A\,^2\Sigma^+$ band at 6000 Å (previously[7]) ascribed to NO$^+$) and the $D\,^2\Sigma^+$–$A\,^2\Sigma^+$ band (11000 Å) have been analysed by FEAST[3]). Similar bands at 5400 Å[8]), at 9690 Å[3]) and between 10000 and 10650 Å[3])[4]) were interpreted[9]), solely on the basis of their wavelengths, as belonging to transitions between previously observed doublet states (H–A, H–C, H–D, F–C). Other groups of bands in the near infrared show great similarity with the $^4\Sigma^-$–$^4\Pi$ bands of the isoelectronic O_2^+ molecule. FEAST, therefore, ascribed them to the analogous transition in NO. Their vibrational structure has been studied by OGAWA[10]) and by BROOK and KAPLAN[11]).

In this paper*) we present a more thorough analysis of the H–A, H–C, H–D and F–C bands. Our investigation is based on recent advances in the interpretation

---

of the NO absorption spectrum reported by LAGERQVIST and MIESCHER[9][12]) and by HUBER and MIESCHER[13]). Without knowing the rotational levels of the combining states, it would hardly be possible to analyze the complex structure of the spectra. Using the data from [9][12][13]) the rotational structure of these bands can be calculated and the correctness of the term assignments can be established by comparison of the calculated and the observed spectrum. The large dispersion in the visible and the infrared, as well as the high rotational temperature of the emission bands allow a more precise determination of molecular constants. For the same reasons it was worthwile to measure and analyse two bands of the $B'-B$ system.

II. Experimental

§ 2. Our light source was similar to the one used by TANAKA and OGAWA[8]): an uncondensed discharge through a rapidly streaming mixture of A and NO. The Π-shaped pyrex discharge tube with Ni electrodes was mounted in 'end-on' position. The A gas between the window and the discharge served as a buffer and was renewed continuously. The NO gas was introduced through a thin glass tube (marked x in fig. 1), in order to avoid its premature dissociation. By regulating the gas supply and the pumping speed, the pressure in the discharge tube was maintained at 15 mm Hg (NO: 11 mm Hg, A: 4 mm Hg). At a current of 90 mA it was possible to suppress almost totally the appearance of the first positive bands of N_2.

Plates of large dispersion were obtained at the 11 m grating spectrograph (600 lines/mm) at the Institute of Physics of the University of Stockholm: the region between 5150 and 6900 Å was photographed in second order with a reciprocal dispersion of 0.7 Å/mm, the region between 7625 and 11 000 Å in first order with 1.4 Å/mm. The exposure times varied with the plates used (Kodak 103a-F; I-N, M, Q, Z) from 1 to $5^1/_2$ hours.

The spectra were measured in comparison with the second and third order iron arc spectrum. The wave number of a single line can be determined with an accuracy of $\pm$ 0.03 cm^{-1}.
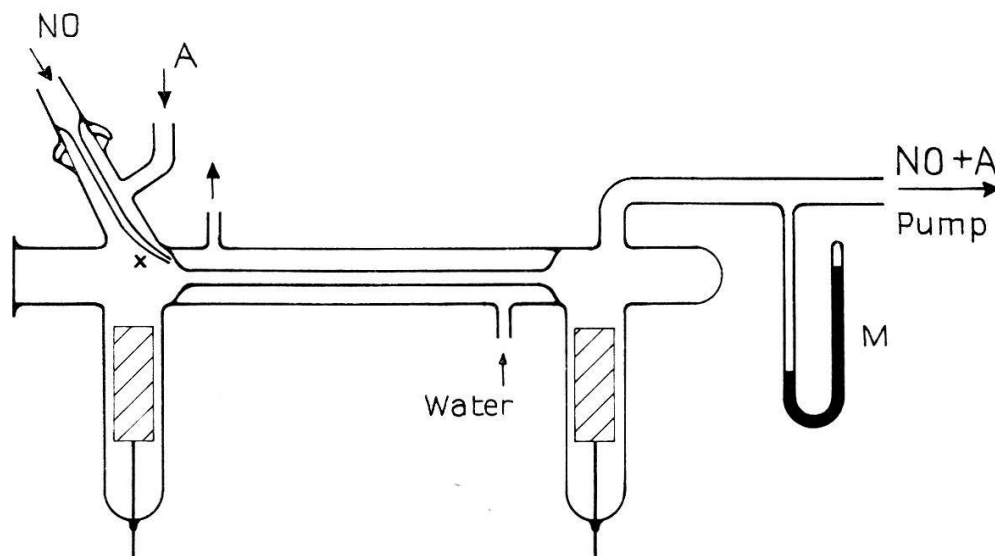

Fig. 1
Discharge tube for the mixture of NO and A gas. Inner diameter 5 mm, length 150 mm.
M: Hg manometer

The spectra show an enormous number of lines, bands frequently overlap; however, over large regions the complex structures are well resolved. Above 6900 Å there are a few A I and O I lines. With the same experimental arrangement we photographed the N_2 spectrum by using N_2 gas instead of NO in the discharge. A comparison of the two exposures shows that our NO plates are free of the lines of the first positive system of N_2 in the relevant wavelength region.

III. Results

§ 3. *Summary.* Fig. 2 shows the emission spectrum of NO between 5000 and 11 000 Å, photographed in small dispersion (glass spectrographs). The notation used indicates two types of band systems:

a) *Rydberg-Rydberg (R-R) Bands.* In the Rydberg states the interaction between the Rydberg electron $\lambda n l$ ($n \geq 3$, principal quantum number, l and λ, quantum numbers of angular momentum and its component on the molecular axis)

Table 1

1	2	3		4	5	6
ℓ'	R'	ℓ'':s	ℓ'':p	R"	λ(Å)	ν_∞(cm⁻¹)
s	E $^2\Sigma^+$	$\sigma 4s$	$\sigma 3s$ / $\pi 3p$ / $\sigma 3p$	A $^2\Sigma^+$ / C $^2\Pi$ / D $^2\Sigma^+$	6000 / 11770 / 13200	16644 / 8497 * / 7572
	S $^2\Sigma^+$	$\sigma 5s$	$\sigma 3s$ / $\pi 3p$ / $\sigma 3p$	A $^2\Sigma^+$ / C $^2\Pi$ / D $^2\Sigma^+$	4359 / 6770 / 7220	22936 * / 14769 * / 13844 *
p	C $^2\Pi$	$\pi 3p \longrightarrow \sigma 3s$		A $^2\Sigma^+$	12240	8167
	D $^2\Sigma^+$	$\sigma 3p \longrightarrow \sigma 3s$		A $^2\Sigma^+$	11000	9092
	K $^2\Pi$	$\pi 4p$	$\sigma 3s$ / $\pi 3p$ / $\sigma 3p$	A $^2\Sigma^+$ / C $^2\Pi$ / D $^2\Sigma^+$	4980 / 8390 / 9090	20091 * / 11924 * / 10630 *
	M $^2\Sigma^+$	$\sigma 4p$	$\sigma 3s$ / $\pi 3p$ / $\sigma 3p$	A $^2\Sigma^+$ / C $^2\Pi$ / D $^2\Sigma^+$	4886 / 8140 / 8800	20460 * / 12293 * / 11368 *
d	F $^2\Delta$	$\delta 3d \longrightarrow$	$\pi 3p$	C $^2\Pi$	10340	9673
	H' $^2\Pi$ / H $^2\Sigma^+$	$\pi 3d$ / $\sigma 3d$	$\sigma 3s$ / $\pi 3p$ / $\sigma 3p$	A $^2\Sigma^+$ / C $^2\Pi$ / D $^2\Sigma^+$	5400 / 9690 / 10620	18506/18 / 10340/51 / 9414/26
	U	$\delta 4d ? \longrightarrow$	$\pi 3p$	C $^2\Pi$	6525	15320

Notes to table 1
Columns 2 and 4: Upper and lower Rydberg states R' and R'' respectively.
Column 3: Transition of the Rydberg electron.
Column 5: Characteristic wavelength (head or center of band).
Column 6: Calculated ν_{00} for transitions not yet observed are marked by *.
Note added in proof: see fig. 2.

and the closed molecular core is small, and for this reason the vibrational and rotational constants of all Rydberg states R are very nearly the same [$\omega(R) \approx 2370$ cm^{-1} $B(R) \approx 2.00$ cm^{-1}]. In the spectrum only the $\Delta v = 0$ sequence appears; its bands all coincide and don't form heads. Normally the separation between the lines is constant, equal to $2B \approx 4$ cm^{-1} in the P and R branches, equal to $B'-B'' \approx 0$ cm^{-1} in the Q branches. However, the structure of the H–R bands (H–A, H–C, H–D) is complicated by the fact that the state H actually consists of two interfering states, H and H'.

b) *Non Rydberg-Non Rydberg (NR-NR) Bands.* In the Non Rydberg (NR) states the vibrational and rotational constants are smaller than in the Rydberg (R) states and they vary from state to state. For this reason the NR-NR bands [B–X (β), B'–B e.g.] are shaded and form sequences which, as a rule, extend over a large wavelength region.

c) The band B'–C (4,1) at 10250 Å belongs to an NR-R transition. It will be shown in § 10 that its appearance is due to a perturbation.

Table 1 gives a summary of the R-R transitions, expected to appear in the photographic region, between the states known from the absorption spectrum of NO. In addition to the R-R bands shown in fig. 2, bands corresponding to the transitions E–D and C–A (FEAST[3]), HEATH[4])) have been observed above 12000 Å. The states N and O (cf. fig. 2) not reported before will be discussed in § 12.

§ 4. *Analysis of the (3d) R-R Bands.* In the complex structures of the H, H'–A, C, D and F–C bands a few of the many superimposed branches can easily be isolated (fig. 3). It is not possible, however, by using the first or second combination differences of one of the combining states to find a correlation between these branches or to discover new branches. On the other hand, the rotational levels of the combining states are known from absorption spectra. The J-numbering in the branches, therefore, can be found by comparing calculated and observed wave numbers of the lines. The numbering is unique, if the error in the calculated wave numbers is smaller than the difference of two consecutive lines of the particular branch. Confirmation is obtained, if e.g. a known local perturbation in a state (i.e. single displaced levels) is observed at the correct J-value or if lines in different bands with common upper state are weakened at the same J'-value.

If the lines of a particular branch are very closely spaced, unique numbering is not possible. However, one can still decide whether a particular branch appears or not.

§ 5. *The Bands H, H'–R.* The upper state consists of two R-states H $^2\Sigma^+$ and H' $^2\Pi$ separated by only 12 cm^{-1}. They interact with each other and produce the level diagram (fig. 4) showing the large Λ-type doubling of the Π state[13]) (the small doublet splittings have been averaged over). The separation between H $^2\Sigma^+$ and H' $^2\Pi_d$ increases linearly with N whereas H' $^2\Pi_c$ is normal. The slope γ of the straight line through the points of fig. 4 is $\gamma = \pm 5.3$ cm^{-1} for H' $^2\Pi_d$ and H $^2\Sigma^+$ respectively.

The anomalous N dependence of the rotational energy in H and H' manifests itself in a characteristic manner in the fine structure of the H, H'–R bands. The Π_c–R sub-bands consist of branches with equidistant lines similar to the branches of the E–A and D–A bands. In the R and P branches the line separation is equal to
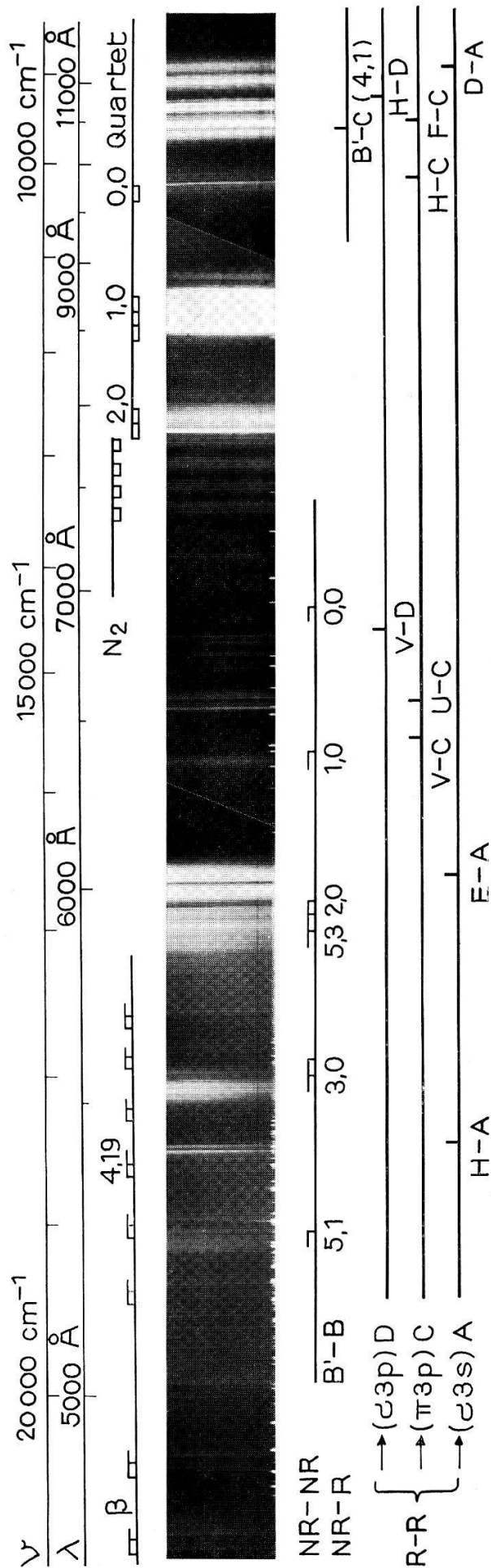
Fig. 2

Emission spectrum of NO (glass spectrographs)

Note added in proof: In table 1 and fig. 2 the letters U and V should be changed to N and O respectively

ν 9500 cm⁻¹   490   480   470   460   9450 cm⁻¹   440   430   420   410   9400 cm⁻¹   390   380

$\Pi - \Sigma$ $\Sigma - \Sigma$ H, H'–D (1,1) $\Sigma - \Sigma$ 11

(P_{11})
(P_{22})

dP_{11} | R$_{11}$
dP_{22} | R$_{22}$
cQ

$(d R_{11})$
$(d R_{22})$

$\boxed{\Pi - \Sigma}$

H, H'–D; H, H'–A (0,0)

R$_{11}$
R$_{22}$
d P$_{11}$
d P$_{22}$
cQ$_{11}$
cQ$_{22}$

ν 590   580   570   18 550 cm⁻¹   540   530   520   510   500   490   480 cm⁻¹

$\boxed{\Sigma - \Sigma}$ H, H'–A (1,1) $\boxed{\Pi - \Sigma}$ $\boxed{\Sigma - \Sigma}$

β(4.19)

d P | R$_{11}$
c Q | R$_{22}$
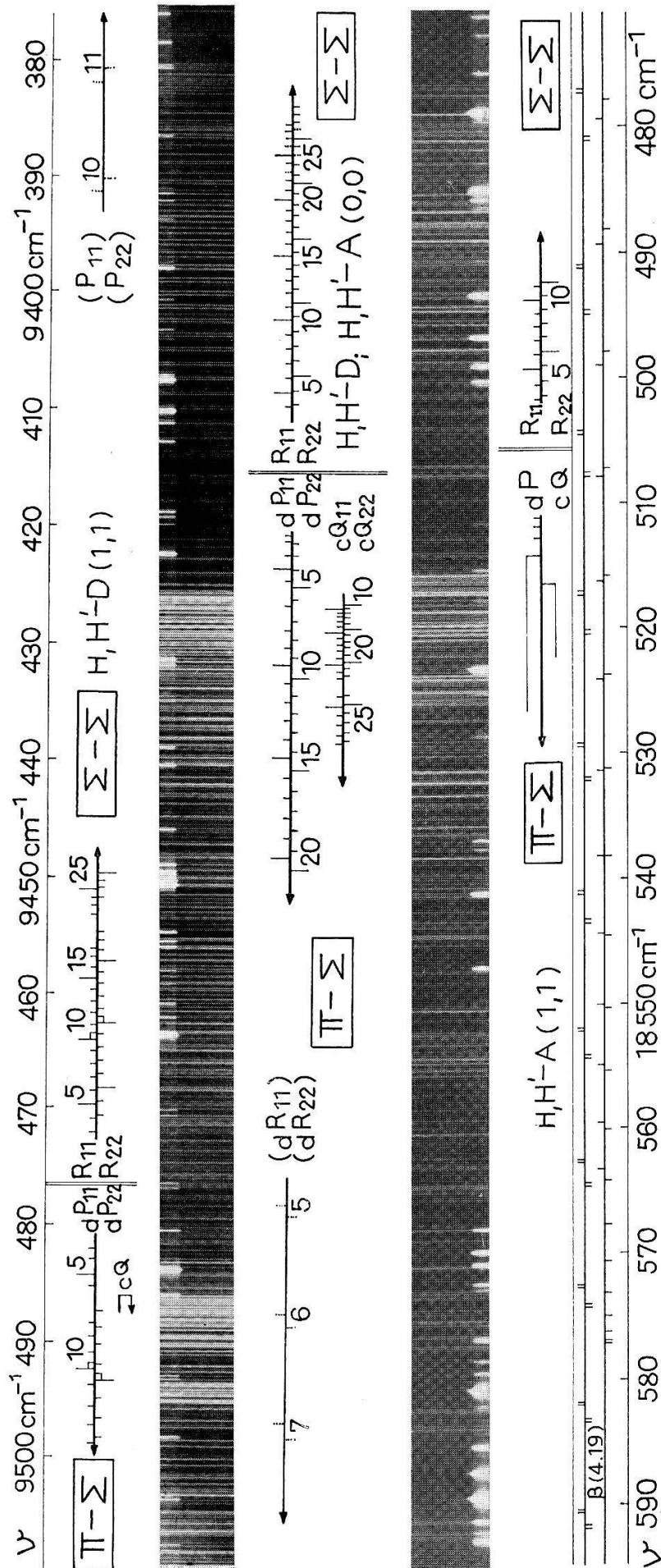
Systems H, H'–D and H, H'–A, matched to common labeling (middle) for the two (0,0) bands. (1,1) bands labeled above and below the spectra concerned. The positions of missing branches are marked (e. g. $H'^2\Pi_d$–$D\,^2\Sigma^+$, $_dR_{11}$ and $_dR_{22}$)
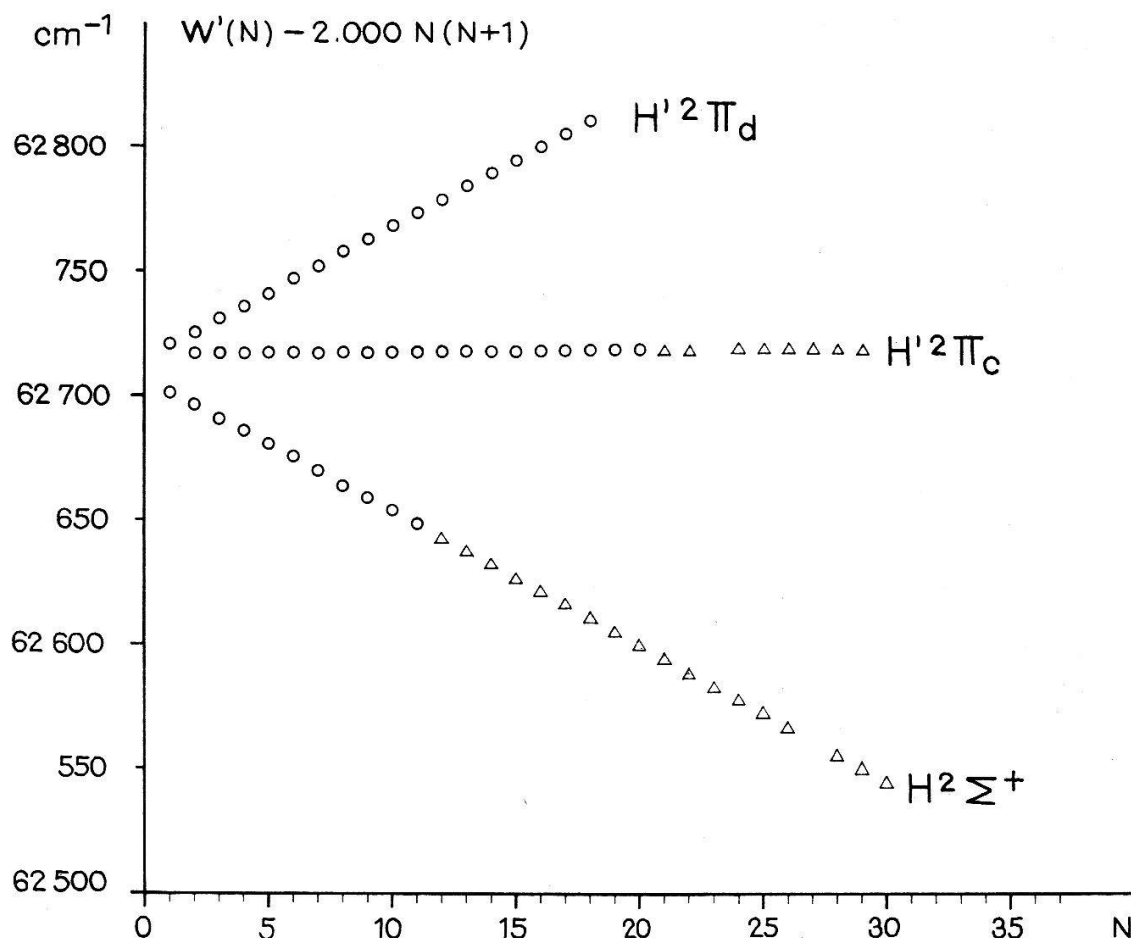
Fig. 4

Level diagram of $H\,{}^2\Sigma^+$ and $H'\,{}^2\Pi$, $v = 0$. The rotational energy $B\,N(N + 1)$, $B = 2.000$ cm^{-1}, is subtracted from total energy $W'(N)$. ○ values from HUBER and MIESCHER[13]), △ values from present analysis

$2\,B \approx 4$ cm^{-1}, all Q lines nearly coincide. In the Π_d–R and Σ–R sub-bands the lines are again equidistant, but here the line separations are $2\,B + \gamma$, γ, $-\,2\,B + \gamma$ in the R, Q, P branches respectively. With the above value of γ the ratio of the line separation in the P and R branches is $9 : 1$ the numbering in the R branches of Σ–R as well as in the P branches of Π_d–R being reversed. The interaction $H \sim H'$, therefore, produces a band structure very different from the pattern of a normal R-R band.

According to the symmetry selection rules for the rotational levels one expects the following branches: in H, H'–A and H, H'–D (lower state Σ^+) R and P branches for Σ–Σ and Π_d–Σ sub-bands, and only Q branches in the Π_c–Σ sub-band; in H, H'–C (lower state Π) R and P branches in Σ–Π_d, Π_c–Π_c, Π_d–Π_d sub-bands, and only Q branches in Σ–Π_c, Π_c–Π_d, Π_d-Π_c sub-bands.

§ 6. $H\,{}^2\Sigma^+$–$D\,{}^2\Sigma^+$, $H'\,{}^2\Pi$–$D\,{}^2\Sigma^+$ (10620 Å). The upper part of fig. 3 shows the bands H, H'–D photographed with the grating spectrograph. The (1,1) band is shifted from (0,0) by 60 cm^{-1} towards shorter wavelengths, $\Delta G_{\frac{1}{2}} = 2339$ cm^{-1} of H and H' being 60 cm^{-1} larger than $\Delta G_{\frac{1}{2}} = 2279$ cm^{-1} of D. The progressing of the branches is clearly visible in this figure. The lines of the strong Q branches of ${}^2\Pi_c$–${}^2\Sigma^+$ (marked $_cQ_{11}$, $_cQ_{22}$) nearly coincide and form the heads at 10606 Å (0,0)

and $10\,540$ Å (1,1). They are partly superimposed on the P branches of $^2\Pi_d-^2\Sigma^+$ (marked $_aP_{11}$, $_aP_{22}$) which progress to the violet. The R branches of $^2\Sigma^+-^2\Sigma^+$ which progress in the opposite direction are free of superimposing lines in the (0,0) band and are therefore easily recognizable. Table 2 gives the measured wave numbers of the lines of these branches with exception of the Q lines of (1,1) which, though separated in the spectrum, are too closely spaced to permit an unique assignment of J-values.

The expected R branches of $^2\Pi_d-^2\Sigma^+$ and the P branches of $^2\Sigma^+-^2\Sigma^+$ are not observed, a fact which will be discussed in § 9. Also branches with mixed indices

Table 2

$H^2\Sigma^+$, $H'^2\Pi-D^2\Sigma^+$ bands, measured wave numbers in cm⁻¹

N	$H^2\Sigma^+ - D^2\Sigma^+$ (0,0)		$H'^2\Pi_c - D^2\Sigma^+$ (0,0)		$H'^2\Pi_d - D^2\Sigma^+$ (0,0)		$H^2\Sigma^+ - D^2\Sigma^+$ (1,1)		$H'^2\Pi_d - D^2\Sigma^+$ (1,1)		N
	R_{11}	R_{22}	Q_{11}	Q_{22}	P_{11}	P_{22}	R_{11}	R_{22}	P_{11}	P_{22}	
0											0
1											1
2	9412.95	9411.51			9421.56	9422.16	9472.07	9470.60	9482.09		2
3	11.78	10.31			21.97	23.21*	70.85	69.39	83.13		3
4	10.54	09.12			23.21*	24.37*	69.67	68.18	84.27		4
5	09.30	07.83			24.37*	25.91	68.44	67.02	85.28		5
6	08.04	06.60					67.27	65.82			6
7	06.80	05.37					66.08	64.67			7
8	05.59	04.14					64.96	63.55			8
9	04.39	02.95			31.12*	31.96*	64.01 e	62.6 e	91.07	9492.11*	9
10	03.21	01.77	9427.78*	9427.34*	32.58*	33.81*	64.01 e	62.6 e	92.51 e	93.46 e	10
11	02.06	00.62	28.15*	27.78*	34.16	35.2*	62.70	61.24	94.09*	95.03*	11
12	00.92	399.48	28.51*	28.15*	35.76	36.78	61.62	60.21	95.68	96.71	12
13	399.82	98.38	28.89	28.58	37.34	38.42	60.62	59.16	97.29	98.41	13
14	98.74	97.31	29.34	29.05	38.98	40.09	59.64	58.21	98.94	500.03	14
15	97.68	96.26	29.81	29.52	40.7 *	41.75	58.57	57.35	500.58	01.66	15
16	96.68	95.30	30.28	30.04	42.32	43.42	57.74	56.27	02.17	03.16	16
17	95.68	94.25	30.82	30.58	44.01	45.10	56.85	55.45			17
18	94.72	93.29	31.37	31.12*	45.73w	46.83w	56.06	54.68			18
19	93.78	92.36	31.96*	31.71	47.43	48.54					19
20	92.89	91.46	32.58*	32.34	49.15	50.26					20
21	92.04	90.60	33.19	32.95							21
22	91.21	89.77	33.41*	33.57			53.21	51.73			22
23	90.42w	88.99w	m	m			52.41	50.84			23
24	89.61	88.23	35.36*	35.13*			51.73	50.26			24
25	88.99*	87.61	36.14	35.93*			51.00	49.62			25
26	m	m	36.91	36.71							26
27	87.61	86.19	37.71	37.50		e: extra lines		e: extra lines			27
28	86.99	85.54	38.56	38.34		$H^2\Sigma^+ - A^2\Sigma^+$ (1,5)		$H'^2\Pi_d - A^2\Sigma^+$ (1,5)			28
29	86.44	84.96	39.39	39.11			9463.40	9462.0 *	51.73 / 9491.93*	9492.87	10

Notes to tables 2, 4, 5, 7, 8 and 9: * blended line; w weak line; m missing line

Table 3

$H^2\Sigma^+$, $v = 0$ and 1, rotational levels in cm⁻¹

N	F'_1, v = 0		F'_2, v = 0		F'_1, v = 1		F'_2, v = 1		N
	from H-X	from H-D	from H-X	from H-D	from H-X	from H-D	from H-X	from H-D	
0									0
1	0.6		- 0.9		0.7		- 0.8		1
2	3.7		2.3		3.9		2.4		2
3	10.7	10.60	9.2	9.16	10.7		9.2		3
4	21.4	21.39	19.9	19.92	21.4	21.41	19.8	19.94	4
5	36.1	36.04	34.6	34.62	36.0	35.92	34.4	34.56	5
6	54.7	54.73	53.3	53.26	54.4	54.45	52.9	52.96	6
7	77.4	77.36	75.9	75.92	76.9	76.85	75.3	75.43	7
8	104.0	103.99	102.6	102.56	103.2	103.10	101.7	101.79	8
9	134.7	134.61	133.1	133.16	133.6	133.54	132.0	132.13	9
10	169.3	169.21	167.7	167.77	167.9	167.82	166.3	166.41	10
11	207.9	207.82	206.3	206.38		206.07	204.8	204.7	11
12		250.44		249.00		248.30		246.84	12
13		297.07		295.63		294.41		293.00	13
14		347.65		346.21		344.52		343.06	14
15		402.23		400.80		398.60		397.17	15
16		460.83		459.41		456.61		455.29	16
17		523.43		522.05		518.56		517.09	17
18		590.01		588.58		584.44		583.04	18
19		660.59		659.16		654.28		652.90	19
20		735.13		733.71					20
21		813.68		812.25					21
22		896.22		894.78					22
23		982.73		981.29		974.41		972.93	23
24		1073.21		1071.78		1063.65		1062.08	24
25		167.64		166.26		167.06		155.59	25
26		266.18		264.80		254.35		254.97	26
27									27
28		1474.92		1473.50					28
29		585.26		583.81					29

Note to table 3: The rotational levels $F'_{1,2}$ give the energy above (or below) $T_0 = W'_1(N = 0)$ of $H^2\Sigma^+$, $v = 0$ ($T_0 = 62\,705.5$ cm⁻¹) and $v = 1$ ($T_0 = 65\,044.9$ cm⁻¹). Addition of T_0 and $F'_{1,2}$ yields the energy above $X^2\Pi_{\frac{1}{2}}$, $J = \frac{1}{2}$, $v = 0$

(e.g. R_{12}, R_{21}) do not occur in accordance with the selection rule $\Delta J = \Delta N$ for Hund's case b. The doublet splittings of H and H' are too small to produce an observable breakdown of this selection rule.

Fig. 5 shows the doublet separations in the R, Q, P branches of the H, H'–D bands (•) as a function of the quantum number N of the upper states.

Rotational levels of $H\ ^2\Sigma^+$ are given in table 3. A comparison with the values resulting from the H–X system shows that the levels are now known with higher accuracy and up to higher quantum numbers N.
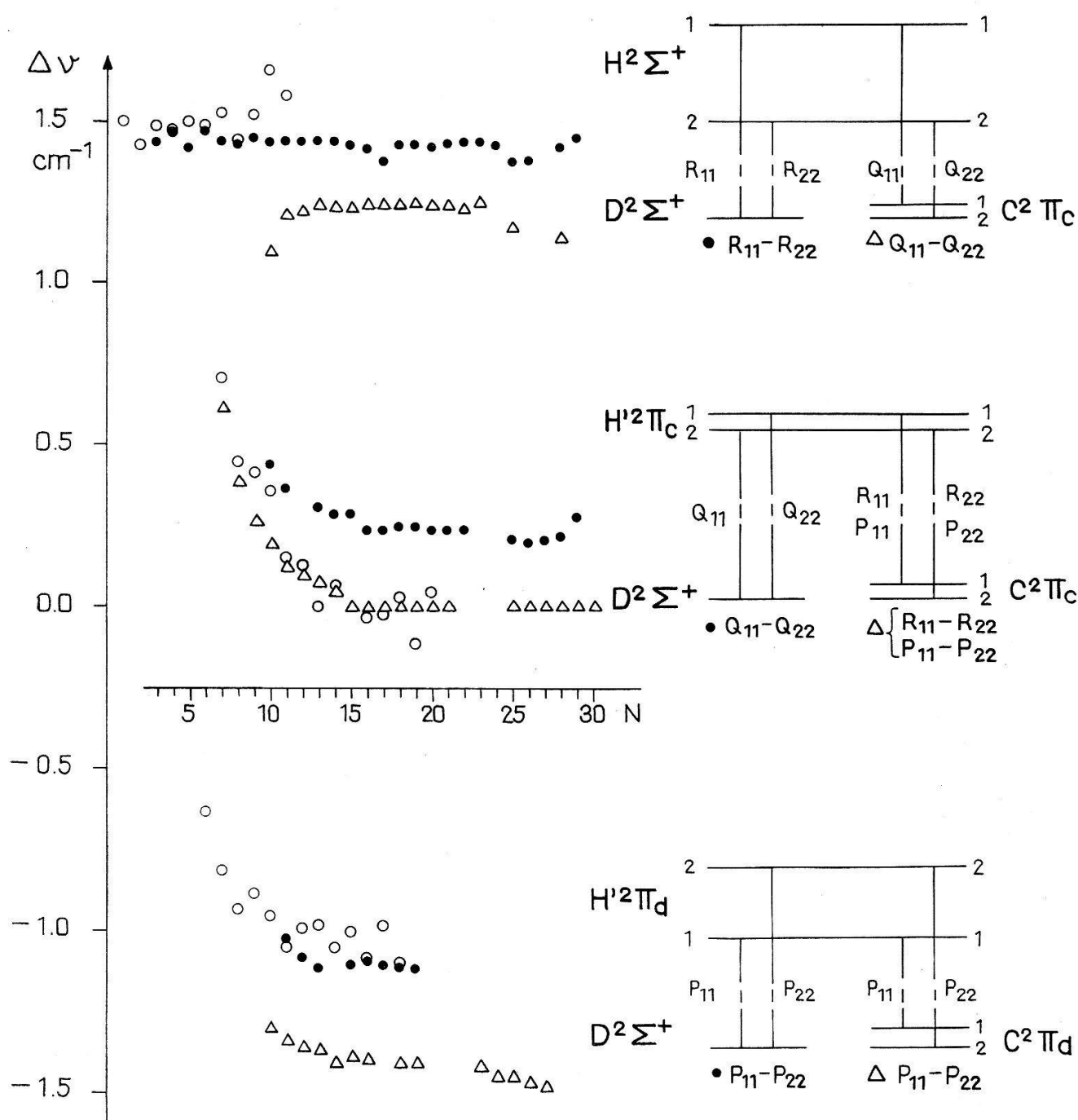

Fig. 5

Doublet splittings of the lines in the H, H'–D (•) and H, H'–C (△) band and of the levels in the H, H' states (○, calculated from H, H'–X [13]). N is the rotational quantum number of the H, H' states

As can be seen from fig. 3 the R-branch in $H\,{}^2\Sigma^+\!\!-\!D\,{}^2\Sigma^+$ (0,0) is so strongly perturbed for $N > 29$, that unique numbering of the lines is not possible. The accumulation of the lines in small dispersion produces the characteristic head at 10657 Å. In the D state small perturbations only are observed for $N > 29$ (shifts not larger than 0.11 cm⁻¹). The perturbation in H–D (0,0) must, therefore, be ascribed to the upper state H.

In the four measured branches of H, H'–D (1,1) the lines $N = 10$ are shifted by $+$ 0.15 cm⁻¹ from their unperturbed position. This shift is due to the interaction between $D\,{}^2\Sigma^+$, $v = 1$ and $A\,{}^2\Sigma^+$, $v = 5$ which coincide at $N = 10$. It has been previously observed by Barrow and Miescher[17] in the $\varepsilon(1,0)$ band. The perturbation gives rise to the appearance of the extra lines R_{11}, R_{22}, P_{11}, P_{22} marked e in table 2. In the same band another perturbation occurs at $N = 19$, 20 and 21. A corresponding perturbation has been observed in D–A; it is due to an interaction of $D\,{}^2\Sigma^+$, $v = 1$ with $B\,{}^2\Pi$, $v = 11$.

The repeated observation of these perturbations is a strong confirmation for the given assignments of the rotational quantum numbers.

Table 4
$H\,{}^2\Sigma^+\!\!-\!A\,{}^2\Sigma^+$ bands, wave numbers in cm⁻¹

N	$H\,{}^2\Sigma^+ - A\,{}^2\Sigma^+$ (0,0) R_{11} measured	diff.	R_{22} measured	diff.	$H\,{}^2\Sigma^+ - A\,{}^2\Sigma^+$ (1,1) R_{11} measured	diff.	R_{22} measured	diff.	N
0									0
1									1
2									2
3									3
4	18502.90	0.14							4
5	01.72	0.13			18499.37	0.03	18497.89*	0.04	5
6					98.19*	0.06	96.74*	0.03	6
7			18497.89*	0.10	97.03*	0.04	95.61*	0.07	7
8	498.19*	0.12	96.74*	0.12	95.92*	0.10	94.50*	0.09	8
9	97.03*	0.09	95.61*	0.11	94.87*	0.15	93.41*	0.11	9
10	95.92*	0.06	94.50*	0.08	93.80*	0.16	92.38*	0.15	10
11	94.87*	0.06	93.41*	0.04	92.66	0.04	91.21*	0.05	11
12	93.80*	-0.01	92.38*	0.01	91.65	0.09	90.15*	0.00	12
13	92.82	0.02	91.38	0.02	90.54*	0.07	89.30*	0.19	13
14	91.92	0.09	90.54*	0.14	89.65*	0.00	88.12*	-0.10	14
15	90.90*	-0.02	89.65*	0.15	88.74*	0.04	87.35	-0.03	15
16	90.15*	0.10	88.74*	0.07			86.97*	-0.07	16
17	89.30*	0.09	87.88*	0.10					17
18	88.45	0.03	86.97*	-0.02					18
19			86.27*	-0.05					19

Note to table 4: diff. = difference between measured and calculated line

§ 7. $H\,{}^2\Sigma^+\!\!-\!A\,{}^2\Sigma^+$, $H'\,{}^2\Pi\!-\!A\,{}^2\Sigma^+$ (5400 Å). The lower part of fig. 3 shows the bands of H, H'–A obtained in an exposure with the grating spectrograph. Superimposed are lines of the $\beta(4,19)$ band. H, H'–A (0,0) and (1,1) nearly coincide. (1,1) is shifted from (0,0) by only 3 cm⁻¹ towards longer wavelengths (for $A\,{}^2\Sigma^+$ $\Delta G_{\frac{1}{2}}$ is equal to 2342 cm⁻¹, for H, H' 2339 cm⁻¹).

In fig. 3 a single labeling could be used for the (0,0) bands of H, H'–A and H, H'–D, as the rotational structure of the two bands is nearly identical. The R branches of the H–A (0,0) band appear particularly strong between $N = 7$ and $N = 12$. This is due to a coincidence with the lines $N = 5$ to $N = 10$ of the H–A (1,1) band.

Table 4 gives the measured wave numbers of the lines of H–A (0,0) and (1,1). Calculated wave numbers were obtained by using the information we have about the rotational structure of the H, H'–D (§ 6) and the D–A[15]) bands. These bands lie

in the infrared and their lines are known with an accuracy of 0.1 cm⁻¹. Table 4 shows furthermore that the agreement between the calculated and the observed wavenumbers is satisfactory, only a small systematic deviation of 0.07 cm⁻¹, between calculated and observed wavenumbers is left.

§ 8. $H\,^2\Sigma^+ - C\,^2\Pi$, $H'\,^2\Pi - C\,^2\Pi$ (9700 Å). The $H, H'-C$ bands show a complex structure with a strong head at 10318 cm⁻¹ and weaker heads at 10350 cm⁻¹ and 10321 cm⁻¹. Again the (0,0) and the (1,1) bands nearly coincide. In addition, the (0,0) group of the NO quartet system is superimposed on these bands.

Table 5 gives the observed wavenumbers of the $H, H'-C$ (0,0) band. The Q branches of the sub-band $^2\Sigma^+ - ^2\Pi_c$ progress with increasing N towards longer wavelengths with the line distance γ and can easily be identified and measured. The R lines of $^2\Sigma^+ - ^2\Pi_d$ form the head at 10318 cm⁻¹ and, therefore, cannot be uniquely associated with quantum numbers. No corresponding P branches can be observed. The transition $^2\Pi_c - ^2\Pi_c$ which has the unperturbed $H'\,^2\Pi_c$ as the upper level shows the symmetrical structure of the E-A and D-A bands, complicated, however, by

Table 5

$H\,^2\Sigma^+$, $H'\,^2\Pi - C\,^2\Pi$ (0,0), measured wave numbers in cm⁻¹

N	$H\,^2\Sigma^+ - C\,^2\Pi_c$		$^2\Sigma^+ - ^2\Pi_d$	$H'\,^2\Pi_c - C\,^2\Pi_c$				$H'\,^2\Pi_d - C\,^2\Pi_c$		$H'\,^2\Pi_d - C\,^2\Pi_d$		N
	Q_{11}	Q_{22}	R_{11} & R_{22}	R_{11}	R_{22}	P_{11}	P_{22}	Q_{11}	Q_{22}	P_{11}	P_{22}	
8						316.26	315.65					8
9						12.57	12.19				356.79	9
10	10285.69	284.59		393.07	392.94	08.86	08.60			357.39	58.69	10
11	80.62	79.41		97.38	97.30	05.17	04.98	404.53*	405.99*	59.31	60.65	11
12	75.43	74.21		401.70	401.63	01.34	01.22	10.17	11.45	61.28	62.64	12
13	70.26	69.02		06.03	05.99	297.83	297.71	15.71	17.01	63.30	64.67	13
14	65.10	63.97			410.38	94.19	94.10	21.25	22.56	65.35	66.76	14
15	59.96	58.73			14.77	90.56	90.50	26.81	28.09	67.42	68.81	15
16	54.85	53.61	head at 10318 cm⁻¹		19.14	286.95		32.39*	33.66	69.54	70.94	16
17	49.77	48.53			23.55	83.38		m	m	71.73w	73.01w	17
18	44.71	43.47			27.97	79.85		43.48	44.77	73.89	75.30	18
19	39.67	38.42			32.39*	76.26		49.03		76.12	77.53	19
20	34.65	33.41			36.84	72.79				78.34	80.03	20
21	29.66	28.42			41.29	69.30				80.82	82.02	21
22	24.71	23.48			45.88	65.83				82.86w	84.58	22
23	19.78	18.53			50.39	62.39				85.49	86.91	23
24	m	m			55.02	58.93				87.89	89.34	24
25	09.97	08.80			59.55	55.69				90.34	91.79	25
26	04.91*	03.83			64.14	52.43				92.84	94.31	26
27	m	m			68.75	49.12				95.40	96.88	27
28	195.65	194.51			73.42	45.91				97.87	99.46	28
29					78.24					400.36	401.95	29
30												30

a small doublet splitting. The Q branches are absent for $^2\Pi_c - ^2\Pi_d$, but have been found for $^2\Pi_d - ^2\Pi_c$. In the $^2\Pi_d - ^2\Pi_d$ sub-bands the P lines are clearly visible. Their corresponding R lines disappear in the background.

The difference in the B values of H and C causes the appearance of a head in the R branches of $^2\Sigma^+ - ^2\Pi_d$ around $N = 20$.

The observed doublet splittings $\Delta\nu$ of the $H, H'-C$ bands are compared in fig. 5 with the corresponding values of $H, H'-D$. As $D\,^2\Sigma^+$ has no measurable doublet splitting the latter values (• in fig. 5) must be approximately equal to the doublet splittings of $H\,^2\Sigma^+$ and $H'\,^2\Pi$. Fig. 5 shows that they agree well with the values known from the $H, H'-X$ bands (○). The doublet splittings of $H, H'-C$ (△ in fig. 5) are somewhat smaller. The differences can be explained by assuming a doublet splitting of 0.2 cm⁻¹ in $C\,^2\Pi_c$ and 0.3 cm⁻¹ in $C\,^2\Pi_d$. These splittings are too small to be observable in the δ bands $(C-X)$ in the vacuum ultraviolet.

The well-known[12]) perturbation in $C\,^2\Pi$, $v = 0$ produced by $B\,^2\Pi$, $v = 7$ would affect the lines of the $H, H'\!-\!C$ (0,0) band at low N values only and, therefore, cannot be observed.

Several lines of the $H, H'\!-\!C$ bands are conspicuously weak or even absent. The analogous phenomena in the $H, H'\!-\!D$ bands*) indicate that there are further perturbations in the H, H' states which are not understood yet. The lines and the levels involved are listed in table 6.

No detailed analysis was carried out for the $H, H'\!-\!C$ (1,1) band. The R lines of $^2\Sigma^+\!-^2\Pi_d$ form the head at $10350\ \mathrm{cm^{-1}}$. The perturbation of the $C\,^2\Pi$, $v = 1$ level by $B\,^2\Pi$, $v = 10$ produces a head ($10321\ \mathrm{cm^{-1}}$) in the P branch of $^2\Pi_c\!-^2\Pi_c$ at $N = 16$.

Table 6

weakened or missing lines		perturbed levels
$\mathrm{H\,^2\Sigma^+ - D\,^2\Sigma^+}$ (0,0)	$\mathrm{H\,^2\Sigma^+ - C\,^2\Pi}$ (0,0)	$\mathrm{H\,^2\Sigma^+}$ v = 0
R(23) R(26)	Q(24) Q(27)	N = 24 N = 27
$\mathrm{H'\,^2\Pi_c - D\,^2\Sigma^+}$ (0,0)	$\mathrm{H'\,^2\Pi_c - C\,^2\Pi}$ (0,0)	$\mathrm{H'\,^2\Pi_c}$ v = 0
Q(18)	R(17),P(19)	N = 18
$\mathrm{H'\,^2\Pi_d - D\,^2\Sigma^+}$ (0,0)	$\mathrm{H'\,^2\Pi_d - C\,^2\Pi}$ (0,0)	$\mathrm{H'\,^2\Pi_d}$ v = 0
P(18)	R(16),P(18) Q(17)	N = 17

§ 9. *Intensities of H, H'–R Bands.* All $H, H'\!-\!R$ bands show the same intensity anomalies. In the bands with the upper state $H\,^2\Sigma^+$ the P branches are unusually weak. In the bands with $H'\,^2\Pi_d$ as an upper state the same holds for the R branches. Only in the bands with the unperturbed $H'\,^2\Pi_c$ as upper state the relative intensities of the branches are normal.

Similar anomalies are known from the H_2 and He_2 spectra[18])[19]). The upper states of the bands in question belong to the $3d$ and $4d$ Rydberg states of these molecules. With increasing rotation of the molecule the coupling between the angular momentum of the d electron and the molecular axis becomes looser (transition to case d).

An interaction between the Σ and Π, Π and Δ states (all in case b) is equivalent to the uncoupling and results in the matrix elements[20])

$$w_{\Sigma,\Pi} = \alpha_{l,\Sigma,\Pi}\sqrt{N(N+1)} \tag{1}$$

$$w_{\Pi,\Delta} = \alpha_{l,\Pi,\Delta}\sqrt{(N-1)(N+2)}, \tag{2}$$

*) Superposition of other lines makes it impossible to observe the same in the H, H'-A bands.

where the parameters α are proportional to the common B value of the three states involved:

$$\alpha_{l,\,\Sigma,\,\Pi} = B \sqrt{l(l+1)}\,, \tag{3}$$

$$\alpha_{l,\,\Pi,\,\Delta} = B \sqrt{l(l+1) - 2}\,. \tag{4}$$

This means that α is considerably smaller for the NO molecule than the corresponding α for H_2 und He_2. Furthermore, two components of its $3d$ complex, $(\sigma\,3\,d)\,H\,^2\Sigma^+$ and $(\pi\,3\,d)\,H'\,^2\Pi$, are only 11.8 cm^{-1} apart from each other, whereas the third one $(\delta\,3\,d)\,F\,^2\Delta$ lies 600 cm^{-1} lower. The l-uncoupling, therefore, affects the rotational levels of the σ and π components only*).

For calculating the relative intensities of the various branches of the H, H'– C, D bands the electron-rotation transition moments tabulated by MacDonald[21]) can be used.

The transition moments A accounting for transitions between unperturbed states are then mixed according to the mixing of the interacting states (in the present case the upper states H and H') resulting in the perturbed transition moments A'

$$A'_{\Sigma-\Sigma} = c_{00}\, A_{\Sigma-\Sigma} + c_{01}\, A_{\Pi-\Sigma}\,, \tag{5}$$

$$A'_{\Pi_d-\Sigma} = c_{10}\, A_{\Sigma-\Sigma} + c_{11}\, A_{\Pi-\Sigma} \tag{6}$$

and

$$A'_{\Sigma-\Pi} = c_{00}\, A_{\Sigma-\Pi} + c_{01}\, A_{\Pi-\Pi}\,, \tag{7}$$

$$A'_{\Pi_d-\Pi} = c_{10}\, A_{\Sigma-\Pi} + c_{11}\, A_{\Pi-\Pi} \tag{8}$$

for lower states of Σ and Π type respectively. The upper state Π_c being unperturbed the resulting $A'_{\Pi_c-\Sigma}$ and $A'_{\Pi_c-\Pi}$ are identical with $A_{\Pi-\Sigma}$ and $A_{\Pi-\Pi}$ respectively.

In the case of the $H \sim H'$ interaction it turns out that the mixture of the Σ and Π_d states is nearly fifty-fifty (for $N = 15$ e.g. 53 : 47). All coefficients c, therefore, have approximately the same magnitude ($\sim 1/\sqrt{2}$). c_{00} and c_{10} have opposite, c_{01} and c_{11} have equal signs. Further, the unperturbed transition moments A which are mixed with each other according to equations (5) to (8) have comparable sizes. For P branches they have equal, but for R branches opposite signs. So the right-hand part of equation (5) results in a difference of two terms of comparable size for P branches and in a sum for R branches. The opposite occurs in equation (6), where

---

*) The interaction between $H\,^2\Sigma^+$, $H'\,^2\Pi$, on the one hand, and $F\,^2\Delta$, on the other hand, is very small indeed. An anomaly, however, is observed, i.e. a slightly too large B value (2.006 cm^{-1} of $H'\,^2\Pi_c$ as well as a slightly too small B value (1.967 cm^{-1}) of $F\,^2\Delta$. The heterogeneous perturbation actually involves the Σ^+, Π_d and Δ_c and on the other hand the Π_c and Δ_d states. The latter case with two interacting states (Π_c and Δ_d) only can be treated in the same manner as the perturbation between $H\,^2\Sigma^+$ and $H'\,^2\Pi_d$ is treated by Huber and Miescher[13]), but with the matrix element of equation (2). The parameter α turns out to be $\alpha = 3.86$ cm^{-1}, i.e. fits within 4% the theoretical value (3.97 cm^{-1}) which is calculated following equation (4) for a d electron ($l = 2$) and the mean B value of $H'\,^2\Pi_c$ and $F\,^2\Delta$. The small difference between the B values mentioned above is due most likely to this mutual interaction of $H'\,^2\Pi_c$ and $F\,^2\Delta_d$.

The fact that in $F\,^2\Delta$ no Δ-type doubling is observed must be ascribed to the further interaction between the Σ^+, Π_d and Δ_c states resulting in the same shifts of levels for the Δ_c as for the Δ_d state.

the difference stands in the case of R branches and the sum in the case of P branches. The same symmetry relations result from equations (7) and (8). The ratios of A' for R and P branches, consequently, are of the type $|(a + b)/(a - b)|$ or its reciprocal value, where $a \approx b$.

Now, the ratio of intensities of two lines is given by the square ratio of the electron-rotation transition moments A', if the two lines in question have a common upper rotational level. (The FRANK-CONDON factor and the population of the upper state do not enter in this case.) The intensity ratio, then, is so extreme that the weaker of two correlated R and P branches cannot be seen on our plates.

Most of the Q branches occurring in the H, H'–R bands have the unperturbed $H'\ ^2\Pi_c$ as an upper state and, therefore, do not show intensity anomalies. However, the mixing affects the intensity of the Q lines in Π_d–Π_c and Σ–Π_c. The influence on the latter, i.e. a weakening, is not easily checked. But as for the former case, it is obvious that the Q lines of $H'\ ^2\Pi_d$–$C\ ^2\Pi_c$, which in a normal Π–Π transition are observed for low N values only, appear as a result of the mixing of the $H\ ^2\Sigma^+$ and $H'\ ^2\Pi_d$ states.

§ 10. $F\ ^2\Delta$–$C\ ^2\Pi$, $B'\ ^2\Delta_i$–$C\ ^2\Pi$. The region crowded with lines between 10100 Å and 10450 Å contains the bands F–C (0,0) and (1,1) and B'–C (4,1). Its most conspicuous features are a not completely resolved accumulation of lines at 9670 cm⁻¹ and additional irregular and weaker accumulations around 9700 cm⁻¹ and 9750 cm⁻¹. At several places the lines can be arranged in branches. One even recognizes reversing of branches at 9741 cm⁻¹ and 9814 cm⁻¹.

Table 7

$F\ ^2\Delta$–$C\ ^2\Pi$ (0,0), measured wave numbers in cm⁻¹

N	cd R_{44} dc		cd P_{44} dc		cd R_{22} dc		cd P_{22} dc		N
7									7
8	9703.84	9702.74			9704.16	9702.99			8
9	07.63	06.24			07.90	06.47			9
10	11.35	09.64			11.60	09.85			10
11	15.00	12.95	9624.73	9622.44	15.24	13.13	9624.98	9622.68	11
12	18.61	16.18	20.53	18.05	18.86	16.36	20.74	18.23	12
13	22.18	19.36	16.27	13.42	22.40*	19.51	16.49	13.55	13
14	25.69	22.40*	11.96	08.69	25.88	22.55	12.20	08.85	14
15	29.10	25.40	07.64	03.91	29.31	25.49	07.84	04.01	15
16	32.44	28.23	03.25	599.00*	32.64	28.34	03.44	599.11	16
17	35.64	30.89	598.82	95.98	35.83	30.99	599.00*	94.1 *	17
18	38.49	33.22	94.27	88.91	38.68	33.26	94.47	89.04	18
19	40.35	34.48	89.44	83.68	40.61	34.63	89.78	83.75	19
20	36.62	30.05			37.02	30.34			20

The R and P lines of F–C (0,0), given in table 7, were easily found with the help of the second combination differences of the $C\ ^2\Pi$ state which are well-known from the δ bands. There are four R and four P branches corresponding to Λ and spin doubling. The doublet splitting in the cd branches is about 0.1 cm⁻¹ larger than in the dc branches. This corresponds to the unequal spin splitting of $C\ ^2\Pi_d$ and $C\ ^2\Pi_c$ already shown in fig. 5. Q branches form the accumulation of lines at 9670 cm⁻¹. Their intensity (larger than in the R and P branches) supports the interpretation of F as a Δ state.

The perturbation of $C\ ^2\Pi$, $v = 0$ by $B\ ^2\Pi$, $v = 7$ would affect only low N levels and is, therefore, not observed. On the other hand, the mutual interaction between $F\ ^2\Delta$, $v = 0$ and $B'\ ^2\Delta$, $v = 2$ appears very clearly in the F–C (0,0) band and can for the first time be studied in the region where it becomes strongest. It is responsible for the reversal of the R branches at $N = 19$ (9741 cm⁻¹). Fig. 6 shows the

difference $\overline{W}'_{B',v=2}(N) - \overline{W}'_{F,v=0}(N)$ ($\overline{W}$ = average of the two spin components) as a function of $N(N+1)$. The term values $B'\,^2\Delta$, $v = 2$ were calculated from the $B'-B$ (2,0) and $\beta(2,0)$ bands (see § 11). In the unperturbed region a straight line with the slope $B_2(B'\,^2\Delta) - B_0(F\,^2\Delta) = 0.6811$ cm^{-1} is obtained (B_2, $B_0 = B$ values of the vibrational levels 2 and 0 respectively). The location of maximum perturbation at $N = 21$ is given by its intersection with the $N(N+1)$ axis and the
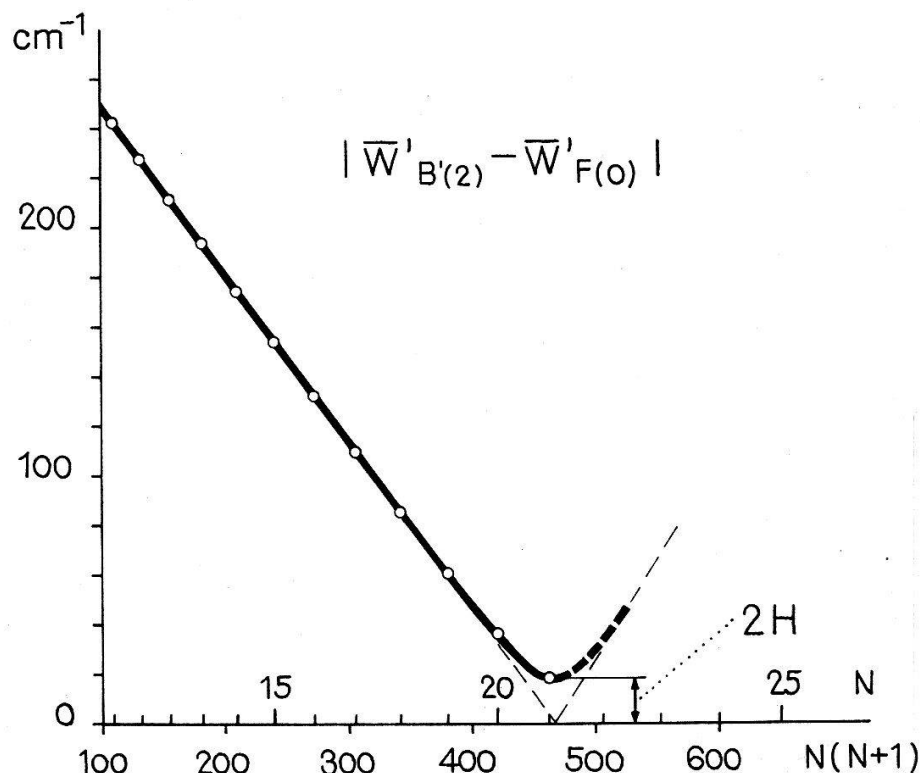
Fig. 6

Perturbation between $B'\,^2\Delta$ $(v = 2)$ and $F\,^2\Delta$ $(v = 0)$

Table 8

$B'\,^2\Delta_i$–$C\,^2\Pi$ (4,1), measured wave numbers in cm^{-1}

N	cd	R_{11}	dc	cc	Q_{11}	dd	cd	R_{21}	dc	cc	Q_{22}	dd	N
8													8
9				9845.84		9847.51*				9847.22		9848.93*	9
10				34.41		36.06				35.79		37.57	10
11				22.24		24.22				23.46		25.53	11
12	9848.93*		9846.63	09.57		11.91	9849.92		9847.51*	10.62		13.02	12
13	40.33		37.65	796.73		799.46	41.14		38.39	797.61		00.44	13
14	32.36		29.31	84.14		87.25	33.01		29.92	84.87		788.04	14
15	25.69		22.24	72.36		75.86	26.20		22.72	72.94		76.49	15
16	20.82		17.08	62.09		65.94	21.24		17.45	62.69		66.47	16
17	18.55		14.59	54.38		58.35	18.87		14.84	54.71		58.76	17
18	19.69		15.68				19.95		15.88				18

minimum value $2H = 18$ cm^{-1} is read from the curve of fig. 6. Therefore, $H = 9$ cm^{-1} results for the interaction parameter. Also an increase of the doublet splitting with N is observed in both the cd and dc branches in F–C, an inverted doublet splitting being produced in $F\,^2\Delta$ by the $B'\,^2\Delta_i$ state.

The F–C (1,1) band coincides with the (0,0) band as the vibrational perturbations[12)22)] produced by B', $v = 4$ in the upper F, $v = 1$ and by B, $v = 10$ in the lower C, $v = 1$ state are accidentally of the same magnitude. Due to the first of these interactions the R branches reverse already at $N \approx 10$ and form the accumulation of lines at 9700 cm^{-1}. The perturbation in this case extends over the whole

band such that the extra lines (wave numbers in table 8) form branches of an 'extra band' $B'-C$ (4,1). The Q branches of this band as well as the somewhat weaker R branches are clearly visible. The P branches, however, are lost in the background. For low N values both branches progress towards longer wavelengths. The R lines reverse at the highest observed N values (9814 cm^{-1}), the Q lines accumulate at 9750 cm^{-1}. An irregular increase in the Λ-type splitting occurs for $N > 16$ and corresponds to the Λ doubling in C $^2\Pi$, $v = 1$ (see [22]) fig. 10). 'Extra bands' $B'-B$ (4,10) and $F-B$ (1,10) are not observed.

§ 11. *The System* B' $^2\Delta_i-B$ $^2\Pi$. OGAWA and SHIMAUCHI[23]) have made an attempt to calculate the B values of the B' state with a higher accuracy than was known from the uv emission spectrum. For this they had to use exposures in which the bands of the $B'-B$ system were not completely resolved. In our pictures these bands are completely resolved and the (1,0) and the (2,0) bands can be analyzed without difficulty. They form the beginning of sequences and their branches can be followed easily up to $J \approx 35$ and $J \approx 20$ respectively, where they become superimposed on the following band of the sequences, (2,1) and (3,1) respectively. The lines of the (1,0) band are given in table 9. Structure and intensities of the $B'-B$ bands are similar to the $B'-X$ bands[24]). Their common state B' $^2\Delta_i$ has a small inverted doublet splitting ($A = -2.4$ cm^{-1}) which decreases rapidly with increasing rotation. In the lower states which have a larger doublet splitting ($A = 30$ cm^{-1} for B $^2\Pi$, $A = 120$ cm^{-1} for X $^2\Pi$) the transition to HUND's case b takes place more slowly. For small J the branches with mixed indices ($R_{12}, Q_{12}, P_{12}; R_{21}, Q_{21}, P_{21}$) are strong in accordance with the selection rule $\Delta\Sigma = 0$ (Σ = quantum number of component of electron spin in direction of the molecular axis). For large quantum numbers the branches with equal indices ($R_{11}, Q_{11}, P_{11}; R_{22}, Q_{22}, P_{22}$) are strong due to the selection rule $\Delta J = \Delta N$. For intermediate values of J all 12 branches

Table 9

B' $^2\Delta_i-B$ $^2\Pi$ (1,0), wave numbers in cm^{-1}

$J-\tfrac12$	cd R_{44}	dc	dd Q_{44}	cc	cd P_{44}	dc	R_{24}	Q_{24}	P_{24}
0									
1							736.13*		
2							40.80	730.75	
3							45.72*	33.28	723.0
4							51.76	36.33	23.5
5	15737.89						57.97	40.05	24.49
6	42.19				15708.18*		64.63*	43.93	25.98*
7	46.89		15725.98*		07.59*		71.79	48.44	27.76
8	52.06*		28.55		07.59*		79.34	53.40	30.13
9	57.57*		31.46*		08.00		87.31	58.76	32.81
10	63.48		34.80		08.85*		95.73	64.63*	36.13*
11	69.80		38.53		09.88		804.55	70.79	39.70
12	76.53		42.65*		711.38	711.44	13.61*	77.41	43.63*
13	783.57	783.67	47.17		13.35*	13.35*	23.4 *	84.40	48.04*
14	91.07	91.14	52.06*		15.59*	15.75		91.89	
15	98.92	99.01	757.43	757.57*	18.33	18.43			
16	807.06	807.18	62.96	63.09	21.39	21.51			
17	15.74*	15.91*	68.93	69.05	24.85	25.07			
18	24.76*	25.00	75.57	75.69	28.74	28.84			
19	34.23	34.37	82.32	82.46	33.04	33.18			
20	43.95	44.10	89.48	89.63*	37.60	37.73			
21	54.03	54.20	97.01*	97.16*	42.65*	42.65*			
22	64.49	64.6	804.93*	805.07*	47.90	48.04			
23	75.27	75.54*	13.27*	13.27*	53.59	53.77			
24	86.37	86.53	21.78	21.94	59.67	59.82			
25	97.56	97.71	30.66	30.84	66.05	66.22			
26	907.22	907.39	39.67	39.85	72.79	72.98			
27	23.91	24.07	47.15	47.33	79.62	79.77			
28	35.96	36.13	61.62	61.82	84.9 *	85.1 *			
29	48.79	48.98	71.52	71.72	97.16*	97.35*			
30	62.06	62.25	82.18	82.37	804.93*	805.07*			
31	75.73	75.93	93.27	93.49	13.27*	13.61*			
32	89.14	89.99	904.80	905.01	22.34	22.59			
33	004.10	004.31	16.67	16.87					
34			28.89	29.13					
35			41.49	41.70					
36			54.38	54.61					
37			67.64	67.86					

R_{22}	Q_{22}	P_{22}	R_{42}	Q_{42}	P_{42}	$J-\tfrac12$
			15694.71	15688.95*		0
			97.10	88.95*		1
15710.62			99.70*	88.95*		2
15.29			702.49	89.23		3
20.29	15704.86	15691.22	05.52	84.73		4
25.62	07.59*	92.08	08.85*	90.48	15674.66	5
31.46*	10.62	92.51	12.46	91.51	73.37	6
37.25	13.99	93.28	16.35	92.83	71.41	7
43.63*	17.71	94.43*	20.56	94.43*	70.91*	8
50.30	21.76	95.63	25.07	96.39	70.26*	9
57.25	26.16	97.61	29.91	98.65	69.93*	10
64.63	30.89	99.70*	35.07	701.24	69.93*	11
72.30	35.95	702.21	40.57	04.15	70.26*	12
80.36	41.34	05.04	46.38	07.40	70.91*	13
88.68	47.17	08.18*	52.54	10.99		14
97.35*	53.23	11.75		14.90		15
806.38	59.67*	15.59*		19.08		16
15.74*	66.47	19.78				17
25.43*	73.61	24.33				18
35.46	81.07	29.23				19
45.81	88.87	34.47				20
56.40	97.01*	39.90				21
66.49	805.35	45.72*				22
80.19	13.27*	52.06*				23
91.51	24.76*	57.80				24
903.54	33.88	67.10				25
15.96	43.70	74.03				26
28.75	53.91	81.63				27
41.88	64.49*	89.63*				28
55.36	75.54*	98.08				29
69.17	86.74	806.85				30
83.24	98.38	16.00*				31
97.41	910.27	25.43*				32
	22.33	35.16				33
		45.03				34
						35
						36
						37

appear with similar intensity. All Q branches are stronger than the corresponding R and P branches. The P branches are noticeably weaker than the R branches, as one should expect for a Δ–Π transition.

The R_{11}, Q_{11}, P_{11} (but not the R_{22}, Q_{22}, P_{22}) lines show a Λ-type doubling at high J values. As expected, the Λ splitting $(\Delta \nu'_{dc})$ in the Δ state is unobservably small. This can be seen from the combination defects

$$\Delta \nu'_{dc}(J) + \Delta \nu'_{dc}(J+1) = [R_{11dc}(J) - R_{11cd}(J)] - [Q_{11cc}(J) - Q_{11dd}(J)]$$
$$= [Q_{11dd}(J+1) - Q_{11cc}(J+1)] - [P_{11cd}(J+1) - P_{11dc}(J+1)],$$

which turn out to be zero, or directly from the equality of the splitting in the R, P and in the Q branches respectively. The measured splitting is, therefore, due to the splitting of the $B\,{}^2\Pi_{\frac{1}{2}}$ levels. Fig. 7 shows the average splitting of the R_{11}, Q_{11}, P_{11} branches as a function of J. In HUND's case a the Λ-type splitting of a regular ${}^2\Pi_{\frac{1}{2}}$ is expected to increase linearly with J[25]:

$$\Delta \nu_{dc} = W_d - W_c = -p(J + 1/2).$$

Without knowing which levels belong to the c or d type only the absolute value of p can be determined. In the present case we get $|\,p(B\,{}^2\Pi, v = 0)\,| = 0.0064$ cm^{-1}. Results of the analysis of the β and γ systems, however, yield additional information on the sign. For the ground state $X\,{}^2\Pi$ GAYDON[26]) (from the γ bands) gives $p = +0.010$ cm^{-1}, GALLAGHER and JOHNSON[27]) (from the microwave spectrum) give $p = +0.0118$ cm^{-1}. From fig. 8 one sees that in the β bands either the difference (fig. 8a) or the sum (fig. 8b) of the Λ splittings of $B\,{}^2\Pi_{\frac{1}{2}}$ and $X\,{}^2\Pi_{\frac{1}{2}}$ will appear depending of the relative positions of the d and c components in $B\,{}^2\Pi_{\frac{1}{2}}$. According to JENKINS et al.[28]) the splitting in the β bands is given by 0.0146 $(J + 1/2)$ cm^{-1}. Obviously this splitting represents the sum of the splittings of the X and the B state*).
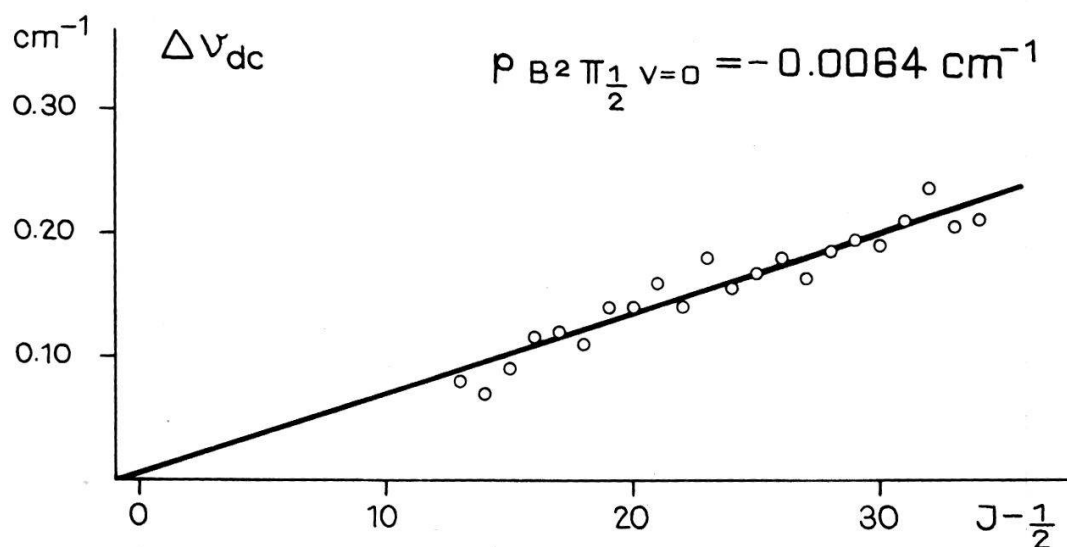
Fig. 7
Λ-type doubling of the $B\,{}^2\Pi_{\frac{1}{2}}$ state

---

*) The result of JENKINS et al. was obtained from $\beta(0,10)$ and $\beta(0,11)$, GAYDON's from $\gamma(0,4)$, GALLAGHER and JOHNSON's from $v'' = 0$. One cannot, therefore, expect an exact fit of the p values.

This strongly suggests that p must be negative:

$$p(B\ ^2\Pi, v = 0) = -\ 0.0064\ \text{cm}^{-1}.$$

With the sign the designations *cc*, *dd*, *cd* and *dc* as used in table 10 follow. Also p being negative the Λ splitting in $B\ ^2\Pi_{\frac{1}{2}}$ cannot be produced by the only known stable $NR\ \Sigma$-state, $G\ ^2\Sigma^-$, because of its negative symmetry.

The band B'–B (1,0) is locally perturbed at $J \approx 23^1/_2$ and $J \approx 27^1/_2$. Fig. 9 shows for $B'\ ^2\Lambda, v = 1$ the variation with $J(J + 1)$ of the levels after subtraction of the unperturbed rotational energy which was calculated according to HILL and VAN VLECK. The Λ splitting observed in the band is not influenced by the perturbation. No extra lines could be identified. By plotting the rotational levels W'_1, W'_2
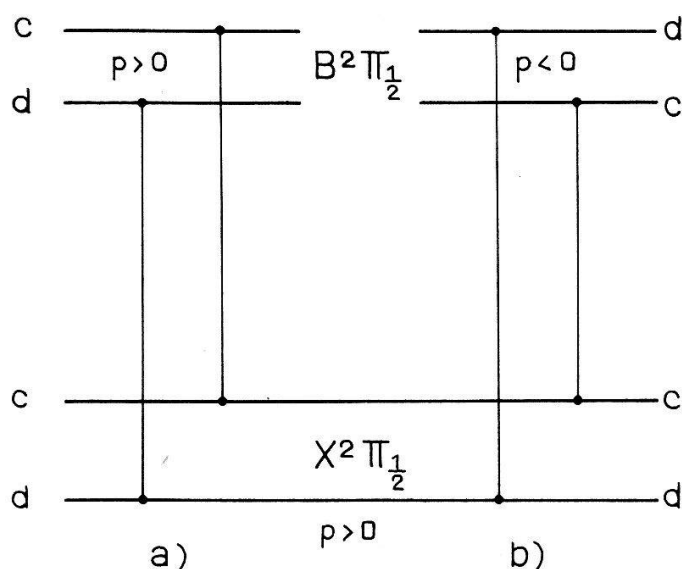
Fig. 8
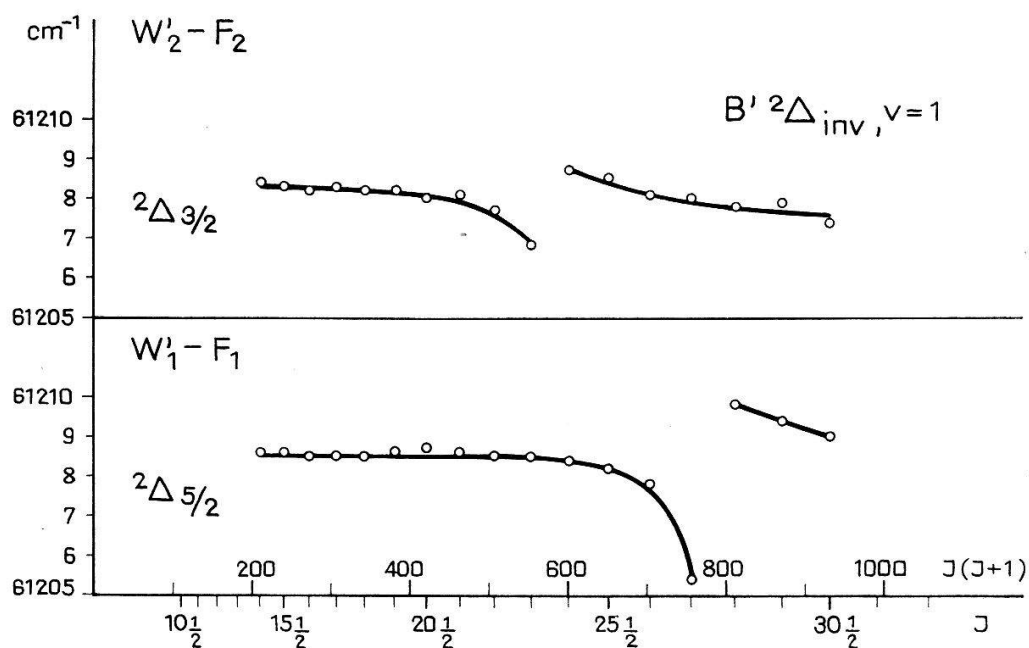
Fig. 9

Perturbation of the rotational structure in $B'\ ^2\Lambda_i$, $v = 1$. The rotational energy F, extrapolated by the HILL, VAN VLECK formula, is subtracted from total energy W'.

as functions of $J(J + 1)$ one can conclude that the perturbations are caused by one component of a doublet state with a $B \approx 1$ cm^{-1}. The term in question could belong to the hitherto unobserved $^2\Phi$ state which in any case would not influence the Λ splitting.

At the highest observed values the lines of the $B'-B$ (2,0) band show the perturbation which is caused by the interaction of the B' $^2\Lambda$, $v = 2$ and F $^2\Lambda$, $v = 0$ levels. This perturbation was already mentioned in the discussion of the $F-C$ (0,0) band (§ 10).

Table 10

Constants of B' $^2\Lambda_i$ (cm^{-1})

B' $^2\Lambda_i$	present * paper	ref. [24])
B_1	1.3021	1.302
B_2	1.282	1.282
D_1	$5.7 \cdot 10^{-6}$	———
D_2	$< 5 \cdot 10^{-6}$	———
$\Delta G_{1\frac{1}{2}}$ *	1153.27	1153.4
A	-2.40**	-2.4

Notes to table 10: * difference between $^2\Lambda_{2\frac{1}{2}}$ ($J = 2\frac{1}{2}$), $v = 2$ and $^2\Lambda_{2\frac{1}{2}}$ ($J = 2\frac{1}{2}$), $v = 1$;
          ** for $v = 1$.

Table 10 gives the constants of the levels B' $^2\Lambda$, $v = 1$ and 2 obtained from the present analysis and a comparison is made with previous results. The D value for $v = 1$ appears normal, for $v = 2$ it is unobservably small; this obviously is a consequence of the mixing of this level with the F, $v = 0$. The coupling constant A was determined graphically from the $B'-B$ (1,0) band using

$$\{F_2' - F_1' + D_1 [(J + 1)^4 - J^4]\}^2 = 4 B_1^2 [(J + 1/2)^2 + Y(Y - 4)] ,$$

(F_1', F_2' = observed rotational energies of the two spin components) plotted as a function of $(J + 1/2)^2$. The resulting straight line intersects the ordinate at $4 B_1^2 Y (Y - 4)$, from which one gets $A = B_1 Y$.

The constants of the lower state B $^2\Pi$, $v = 0$ agree with the values given by JENKINS et al.[28]).

IV. Concluding Remarks

§ 12. The emission of the bands which have been described in this paper requires an excitation energy between 61 000 and 65 500 cm^{-1} which is about 10 000 cm^{-1} higher than the dissociation energy (6.48 eV) of the molecule. As the absorption spectrum (reproduction in [12])) shows, there are vibrational levels of many other R and NR states in the same energy region. It turns out, however, that with our light source the R terms D, E, F, H, H' and the NR term B' are the only ones to occur as upper states of emission bands. The excitation by active nitrogen (TANAKA[29])) does not produce any bands with upper levels above the dissociation limit.

The absence of emission bands with K, M or S (cf. table 1) as upper states can be ascribed to weak predissociation noticeable only in emission or to interactions with other predissociating levels. The branches of the D–A (1,1) (2,2) (3,3) and E–A (2,2) bands break off abruptly, in D–A for energies of $D\ ^2\Sigma^+$, $v = 1$ and 2, at 59270 cm^{-1}, for $v = 3$ at 60100 cm^{-1} and in E–A for $E\ ^2\Sigma^+$, $v = 2$ at 68100 cm^{-1}. It is understandable, therefore, that the respective next-higher $^2\Sigma^+$ R states M and S do not give rise to emission bands. The predissociation is most likely produced by the repulsive $NR\ ^2\Sigma^+$ state originating from unexcited atoms N (^4S) and O (^3P). The state $K\ ^2\Pi$ as well as the next-lower state in the same Rydberg series, $C\ ^2\Pi$, interact strongly with the NR state $B\ ^2\Pi$. $B\ ^2\Pi$ itself is observed as upper state of emission bands only up to $v = 7$ (Deézsi[30]). This interaction presumably will depopulate the C levels for $v > 0$ as well as all K levels.

Three distinct but weak bands in the emission spectrum of NO remain to be explained, namely (cf. fig. 2) N–C (6525 Å), O–C (6409 Å) and O–D (6805 Å). The wave number of the first band (cf. table 1) equals the difference between a state N (observed in absorption as the upper state of the partly analysed 'ϱ-band'[14]) and $C\ ^2\Pi$. The second and the third bands have a distance (910 cm^{-1}) equal to the energy difference of the states D and C and, therefore, might have a common upper state O. N at 67695 cm^{-1} could be ($\delta\ 4\ d$) $^2\Delta$[13]), and the N–C band the second member of the $\delta\ n\ d \rightarrow \pi\ 3\ p$ Rydberg series which starts with F–C. The state O would lie at 67990 cm^{-1}, for $n = 4$ its quantum defect would be $a = 0.03$, close to the corresponding value of H, H' ($a = 0.02$). Most likely O would consist of two interacting states ($\sigma\ 4\ d$) $O\ ^2\Sigma^+$ and ($\pi\ 4\ d$) $O'\ ^2\Pi$ in complete analogy to the H, H' states. Indeed, the fine structure of the O–D and O–C bands which then would form the second members of the Rydberg series $\sigma, \pi\ n\ d \rightarrow \sigma\ 3\ p$ and $\sigma, \pi\ n\ d \rightarrow \pi\ 3\ p$ is extremely complex. As long as more data about O are not available from the absorption spectrum an analysis of the emission bands is not possible.

The appearance of emission bands with $4\ d$ states as upper levels is in agreement with the previous[13]) observation for $3\ d$ states that the d states are hardly perturbed by other states except by $B'\ ^2\Delta$, and that a few single levels (cf. table 6) only, due to resonance with single levels of predissociating states, are absent.

Finally it should be mentioned that $G\ ^2\Sigma^-$–$B\ ^2\Pi$ bands whose upper NR state $G\ ^2\Sigma^-$ is now well known[31]), are not observed, neither are $B'\ ^2\Delta$–$^2\Phi$ bands. The expected low $^2\Phi$ state for the $\sigma^2\ \pi^3\ \pi^2$ configuration still remains undetected.

The present investigations have resulted in a complete interpretation of all doublet band systems of NO observed in emission. The analysis of the infrared quartet system, however, is still lacking. The heads of this system, plainly visible in fig. 2, appear as irregular accumulations of lines on the high dispersion plates. The overlapping doublet bands, strongly emitted by the light source used in this experiment could probably be avoided, if a much milder discharge, e. g. active nitrogen, could be applied to excite the NO in the low $^4\Sigma^-$ state.

Literature

[1] G. GEHLHOFF, Ann. Phys. *24*, 553 (1907).

[2] J. ZENNECK und B. STRASSER, Phys. Z. *12*, 1201 (1911).

[3] M. W. FEAST, Canad. J. Res. A *28*, 488 (1950).

[4] D. F. HEATH, Los Alamos Rep. *2335*, 30 (1960).

[5] W. H. WURSTER, C. E. TREANOR and H. M. THOMPSON, J. Chem. Phys. *37*, 2560 (1962).

[6] P. BAER und E. MIESCHER, Helv. Phys. Acta *26*, 91 (1953).

[7] C. JAUSSERANT, L. GRILLET et M. DUFFIEUX, C. R. *205*, 39 (1937).

[8] Y. TANAKA and M. OGAWA, J. Sci. Res. Inst. Tokyo *44*, No. 1208 (1949).

[9] A. LAGERQVIST and E. MIESCHER, Canad. J. Phys. *40*, 352 (1962).

[10] M. OGAWA, Sci. Light Tokyo *3*, 39 (1954).

[11] M. BROOK and J. KAPLAN, Phys. Rev. *96*, 1540 (1954).

[12] A. LAGERQVIST und E. MIESCHER, Helv. Phys. Acta *31*, 221 (1958).

[13] K. P. HUBER and E. MIESCHER, Helv. Phys. Acta *36*, 257 (1963).

[14] E. MIESCHER, J. Quant. Spectrosc. and Radiat. Transfer *2*, 421 (1962).

[15] D. F. HEATH, private communication (1961).

[16] L. GERÖ and R. SCHMID, Proc. Phys. Soc. *60*, 533 (1948).

[17] R. F. BARROW and E. MIESCHER, Proc. Phys. Soc. [A] *70*, 219 (1957).

[18] P. M. DAVIDSON, Proc. Roy. Soc. [A] *138*, 580 (1932).

[19] G. H. DIEKE, Z. Phys. *57*, 71 (1929).

[20] G. H. DIEKE, Phys. Rev. *47*, 873 (1935).

[21] J. K. L. MACDONALD, Proc. Roy. Soc. [A] *138*, 183 (1932).

[22] A. LAGERQVIST and E. MIESCHER, to appear.

[23] M. OGAWA and M. SHIMAUCHI, Sci. Light Tokyo *5*, 147 (1956).

[24] E. MIESCHER, Helv. Phys. Acta *29*, 401 (1956).

[25] R. S. MULLIKEN and A. CHRISTY, Phys. Rev. *38*, 87 (1931).

[26] A. G. GAYDON, Proc. Phys. Soc. *56*, 160 (1944).

[27] J. J. GALLAGHER and C. M. JOHNSON Phys. Rev. *103*, 1727 (1956).

[28] F. A. JENKINS, H. A. BARTON and R. S. MULLIKEN, Phys. Rev. *30*, 150 (1927).

[29] Y. TANAKA, J. Chem. Phys. *22*, 2045 (1954).

[30] I. DEÉZSI, Acta Phys. Hung. *11*, 155 (1960).

[31] A. LOFTHUS and E. MIESCHER, Canad. J. Phys. *42*, 848 (1964).